Topological nature of the Kondo insulator SmB_6 and its sensitiveness to Sm vacancy

W. K. Park,[1,*] J. A. Sittler,[1,2,†] L. H. Greene,[1,2] W. T. Fuhrman,[3] J. R. Chamorro,[3,4] S. M. Koohpayeh,[3] W. A. Phelan,[3,‡] and T. M. McQueen[3,4,5]

[1]*National High Magnetic Field Laboratory, Florida State University, Tallahassee, Florida 32310, USA*
[2]*Department of Physics, Florida State University, Tallahassee, Florida 32306, USA*
[3]*Institute for Quantum Matter, Department of Physics and Astronomy, Johns Hopkins University, Baltimore, Maryland 21218, USA*
[4]*Department of Chemistry, Johns Hopkins University, Baltimore, Maryland 21218, USA*
[5]*Department of Materials Science and Engineering, Johns Hopkins University, Baltimore, Maryland 21218, USA*

(Received 30 March 2020; revised 4 January 2021; accepted 29 March 2021; published 14 April 2021)

The true topological nature of the Kondo insulator SmB_6 remains to be unveiled. Our previous tunneling study not only found evidence for the existence of surface Dirac fermions, but it also uncovered that they inherently interact with the spin excitons, collective excitations in the bulk. We have extended such a spectroscopic investigation into crystals containing a Sm deficiency. The bulk hybridization gap is found to be insensitive to the deficiency up to 1% studied here, but the surface states in Sm-deficient crystals exhibit quite different temperature evolutions from those in stoichiometric ones. We attribute this to the topological surface states remaining incoherent down to the lowest measurement temperature due to their continued interaction with the spin excitons that remain uncondensed. This result shows that the detailed topological nature of SmB_6 could vary drastically in the presence of disorder in the lattice. This sensitiveness to disorder is seemingly contradictory to the celebrated topological protection, but it can be understood as being due to the intimate interplay between strong correlations and topological effects.

DOI: 10.1103/PhysRevB.103.155125

I. INTRODUCTION

Topological materials defy description by the conventional Landau-Ginzburg paradigm based on broken symmetries [1,2]. Instead, they can be classified by a completely new scheme, namely topological invariants characterizing their band structure. A topological insulator (TI) is insulating in the bulk, but its surface is a robust conductor due to the topological surface states (TSSs) protected by spin-momentum locking [3]. In an f-orbital-based Kondo insulator (KI) [4], strong correlations play a key role in reducing the hybridization gap (HG) by bringing the hybridized band edges close to each other, enhancing the effective mass [5,6]. Then, combined with the inherently large spin-orbit coupling, band inversions can occur at high-symmetry points, possibly transforming the KI into a topological phase, namely TKI [7]. The true nature of TKIs, a representative group of correlated topological phases, remains to be unveiled, posing a big challenge [6,8], in sharp contrast to their weakly correlated counterparts, much of whose underlying physics is now well understood [2].

SmB_6 has been a focus of intensive study recently as a prime candidate for a TKI [6,8]. Although the low-temperature resistance plateau is now firmly established as due to the TSS, the exact topological nature is not known yet, with the origin of quantum oscillations remaining largely controversial [9–12]. This is due to multifaceted challenges, including (i) materials science issues in the bulk [13,14] and/or at the surface (e.g., polar nature) [15,16], and (ii) the intriguing interplay between strong correlations and topology that is not yet well understood. Consequently, despite the early observation of a HG in several spectroscopic studies, including angle-resolved photoemission spectroscopy (ARPES) [17–23], scanning tunneling spectroscopy (STS) [15,24,25], and point-contact spectroscopy (PCS) [26], spectroscopic signatures for the TSSs remained obscure, as discussed in the supplemental material (SM) [27]. Our recent study employing planar tunneling spectroscopy (PTS) [28] has provided clear evidence for the surface Dirac fermions, in good agreement with band calculations [29–32] and a quantum oscillation study [9]. Remarkably, the TSSs were found inherently to interact with the spin excitons (SEs) [33], collective bulk excitations, in agreement with a theoretical [34] and an ARPES [35] studies.

One of the remaining crucial questions is how the topological nature of SmB_6, or TKIs in general, is influenced by a disorder in the (Kondo) lattice. This is a particularly important topic since Sm vacancies are known to occur easily in single crystals grown by the floating-zone (FZ) technique [13,14]. Previously, impurities without f-electrons were speculated to induce in-gap states in the bulk, and thus to be responsible for the low-temperature metallicity [36,37]. However, now that it is known to be due to the TSSs in stoichiometric crystals [6,8],

*Corresponding author: wkpark@magnet.fsu.edu
†Present address: Department of Physics, University of California Santa Cruz, Santa Cruz, CA 95064, USA.
‡Present address: Los Alamos National Laboratory, Los Alamos, Mail Stop E574, Los Alamos, NM 87545, USA.

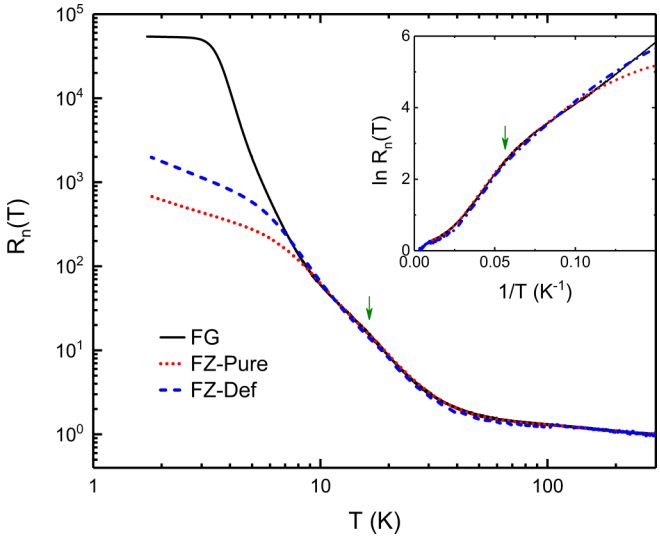

FIG. 1. Normalized dc electrical resistance measured across the (001) surface of three SmB_6 crystals. Double-logarithmic (main panel) and Arrhenius plot (inset) of the normalized resistance, $R_n(T) \equiv R(T)/R(300\,\mathrm{K})$. While they exhibit similarly insulating behaviors at high temperature, a large discrepancy is apparent below ~10 K.

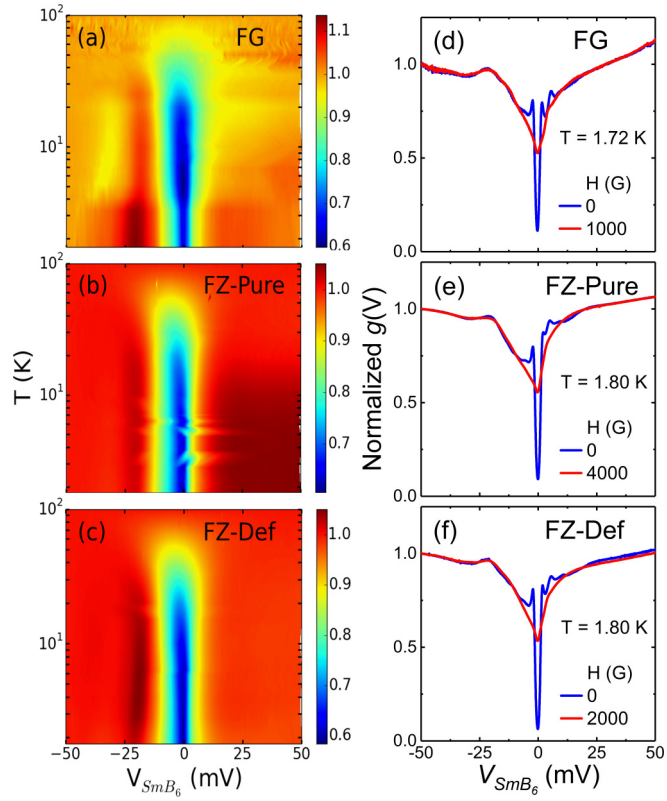

FIG. 2. Bulk HG and the TSS in SmB_6. (a)–(c) Color-contour maps of the normalized tunneling conductance, g(V). Below the T_c (7.2 K) of Pb, conductance was measured with the Pb driven normal by magnetic fields indicated in (d)–(f). Overall, all three crystals exhibit similar features due to the opening of a bulk HG. (d)–(f) Normalized conductance at the lowest temperature with the Pb superconducting (blue solid lines) and driven normal (red solid lines). An additional peak is seen only in the positive-bias branch (5–6 mV).

the role of Sm deficiency needs to be understood more comprehensively by taking the topological aspect into account. More specifically, studying how the SEs evolve with increasing Sm deficiency and consequently how their effect on the TSSs changes may help elucidate the interplay between strong correlations and topology. In this paper, we report a PTS study on Sm-deficient SmB_6 crystals, and we compare it with our previous results from stoichiometric crystals [28,38]. While the bulk HG largely remains the same, the TSSs are found to undergo distinct temperature evolutions due to drastic changes in their interaction with the SEs.

II. RESULTS

The normalized dc electrical resistance, $R_n(T) \equiv R(T)/R(300\,\mathrm{K})$, measured across the polished (001) surface, is plotted in Fig. 1 for three SmB_6 crystals that are also used in our PTS study. One is a stoichiometric flux-grown (FG) crystal studied previously [28,38]. The other two are grown by the floating-zone technique, labeled by the nominal purity of the starting growth material as FZ-Pure and FZ-Def (FZs collectively), respectively. The FZs are known to have Sm vacancies up to 1% [13,14] regardless of the nominal purity, which can be inferred from the similar behaviors they exhibit throughout this study. At high temperature, the three crystals show an almost identically insulating behavior including a broad hump at 15–20 K as marked by the arrow, below which a noticeable slope change occurs (see the inset). The activation-type energy gaps (in meV) extracted from an Arrhenius analysis for the temperature range higher (Δ_h) and lower (Δ_l) than the hump temperature are (Δ_h, Δ_l) = (5.6, 3.1), (5.4, 2.9), and (5.2, 3.3) for the FG, FZ-Pure, and FZ-Def, respectively. Note that below ~10 K, the $R_n(T)$ curves become distinct: While the FG forms a pronounced plateau below ~4 K after a rapid increase by five orders of magnitude [39], the FZs show an increase only by two to three orders of magnitude followed by a mere *slowdown* below ~7 K. This discrepancy is likely to be associated with the Sm deficiency [13,14], but transport studies alone cannot address whether the slowdown in the FZs is still due to the TSSs or the in-gap states.

For spectroscopic investigations into this question, tunnel junctions are prepared by following the same procedure as before with Pb as the counterelectrode [28,38]. It is noteworthy that some of the aforementioned surface issues were resolved by plasma-oxidizing the crystal to form a high-quality B_2O_3 tunnel barrier beneath which the TSSs reform [27]. The differential conductance, $g(\mathrm{V}) \equiv dI/dV$, normalized by the parabolic background at 100 K is shown as color-contour maps in Figs. 2(a)–2(c). In all three crystals, with decreasing temperature, there is a suppression around zero bias below 60–70 K and an enhancement around −20 mV, indicative of the formation of a bulk HG [28] in agreement with an ARPES study [22,27]. Thus, independent of the Sm-deficiency level, a HG of comparable size ($\Delta_{\mathrm{hyb}} = 21$ meV) opens at approximately the same temperature, explaining the similarly insulating behavior in $R_n(T)$ down to ~10 K. Since the bulk

HG is an essential prerequisite for the TSSs in TKIs [7], its robustness against Sm vacancies suggests that the TSSs may still be responsible for the slowdown in FZs. But then why does $R_n(T)$ not form a clear plateau as in the FG? To address this, we first scrutinize g(V) curves at the lowest temperature [Figs. 2(d)–2(f)]. Here, two curves are shown for each crystal, one with the Pb superconducting and the other with it driven normal by applied magnetic fields. In all cases, they overlap well at high bias, as expected, including the broad peak around −20 mV. At low bias, they deviate drastically: sharp Pb coherence peaks (Pb superconducting) versus an overall V-shape (Pb nonsuperconducting), the latter being reminiscent of the density of states (DOS) for Dirac fermions. Such V-shaped, i.e., linear conductance has been reported in STS studies of Bi_2Se_3 [40,41] but is missing in STS [15,24,25] and PCS [26] data on SmB_6. Possible reasons for these discrepant observations are discussed in Sec. 4 of the SM [27]. Notice an additional peak at 5–6 mV appearing *only* in the positive bias branch. Together with the coherence peaks being *asymmetric*, this was a crucial clue to unraveling the topological nature of SmB_6 [28]. Here, we demonstrate that the fine spectroscopic differences among the three crystals indicate the sensitiveness of the TSS to the Sm deficiency.

Normalized g(V) curves with the Pb driven normal are compared in 3(a) in a low-bias region. Two common features appear in the overall V-shaped curves: a broad hump around −2 mV and a kink at +4 mV. Since this hump-kink structure originates from the TSS interacting with the SEs [28], their common observation suggests such interaction still exists in the FZs. A clear difference is also observed: on the positive bias side, there are two distinct slopes for the FG, whereas the curve is just quasilinear for the FZs. The former originates from two distinguishable surface Dirac cones centered at $\bar{\Gamma}$ and $\bar{\chi}$ points in the (001) surface Brillouin zone [28]. Thus, the latter nominally indicates that the two Dirac cones are indistinguishable in the FZs, presumably due to their intermixing. To find the microscopic origin, the conductance at each temperature with the Pb superconducting is normalized by that with it driven normal [Figs. 3(b)–3(d)]. Such normalization effectively divides out the spectral density in SmB_6 and thus would leave only the superconducting Pb features behind. However, additional features are revealed, e.g., in the FG [Fig. 3(b)]: (i) the asymmetry in the coherence peaks (marked by V+ and V−) increases with increasing temperature, and (ii) the peak labeled as V_1 is more clearly visible. These features were shown to originate from the inelastic tunneling involving SEs in SmB_6 [28]. The V_1 peak's Pb phononic origin can be completely ruled out by its independence of the counterelectrode (Sec. 5 in [27]). There are important contrasts among the crystals: (i) In the FZs, the V_1 peak is not as pronounced as in the FG despite the similar temperature dependence of its normalized height [Fig. 3(e)], and (ii) The coherence peaks in the FZs remain asymmetric down to the lowest temperature, whereas they become symmetric below ∼4 K in the FG, as shown more quantitatively in Fig. 3(f) by the normalized peak height getting close to 1 below ∼4 K (see the inset).

The inelastic tunneling features arising from processes occurring in the SmB_6 are more clearly visible when the Pb is superconducting because of the sharp coherence peaks in its

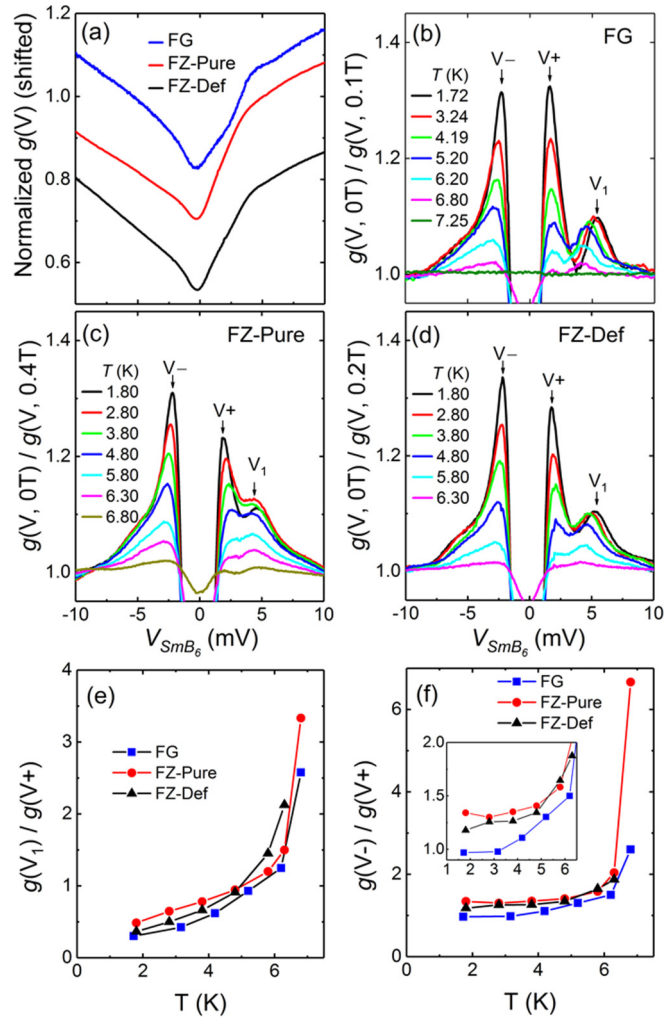

FIG. 3. Influence of the SEs on the TSS. (a) Elastic tunneling effect when the Pb is driven normal. Normalized g(V) shows common features of hump (around −2 mV) and kink (∼4 mV) originating from the interaction with virtual SEs. An apparent discrepancy is two linear slopes (FG) vs quasilinear shape (FZs), possibly due to intermixing of the two surface Dirac cones. (b)–(d) The inelastic tunneling effect is clearly seen when g(V) with the Pb superconducting is divided out by g(V) when the Pb is driven normal by applied magnetic fields. (e) V_1 peak height normalized against the positive-bias coherence peak ($V+$). (f) Height of the negative-bias coherence peak ($V-$) normalized against $V+$;. Inset: a zoomed view for the low-temperature region.

single-particle DOS, thereby increasing the energy resolution (note the tunneling spectrum is a convolution of the Pb and SmB_6 DOS) [28]. The V_1 peak originates from the emission of SEs at $eV = \Delta_{Pb} + \omega_0$, where ω_0 is the characteristic SE energy, and Δ_{Pb} is the superconducting gap energy, at which the *occupied* DOS (i.e., where electrons tunnel from) is peaked. Meanwhile, the contribution from the absorption channel is most pronounced at $eV = -\Delta_{Pb}$ due to the peaked *empty* DOS (i.e., where electrons tunnel into), leading to the coherence-peak asymmetry. Thus, the persistence of the V_1 peak in FZs indicates that the SEs still exist at the lowest measurement temperature. When the Pb is driven normal, the same inelastic tunneling effect must still exist, albeit much

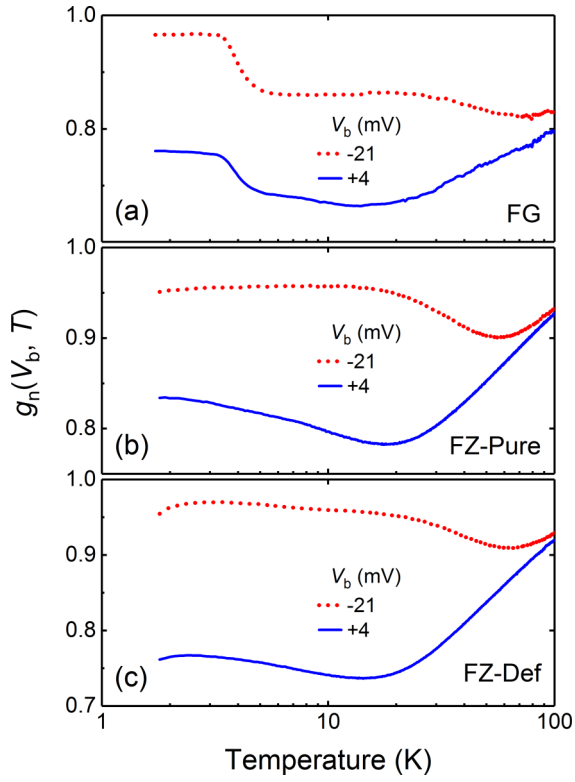

FIG. 4. Temperature evolution of the TSS. (a)–(c) Temperature dependence of conductance at two fixed bias voltages ($V_b = -21$ and $+4$ mV) normalized against -50 mV. At low temperature, while the FG exhibits a rapid increase followed by plateauing, FZs exhibit gradual changes.

weakened due to the lower energy resolution. However, such inelastic tunneling cannot account for the hump-kink structure observed when the Pb is driven normal since, due to the flat DOS, the emission process should cause only a parallel shift of the conductance for $eV \geqslant \omega_0$ and the absorption process can occur without any characteristic energy scale. This indicates that the hump-kink structure appears via elastic tunneling. Thus, it is an intrinsic characteristic of the surface spectral density, modified via the electronic self-energy change due to the exchange of *virtual* SEs [34], analogously to the hump-dip structure in Pb DOS arising from the exchange of virtual phonons [42].

To reveal the underlying microscopic origin for the discrepant behaviors among the three crystals, the conductance is measured at a fixed bias voltage (V_b) over a wide temperature range from 1.8 to 100 K, $g(V_b, T) \equiv \frac{dI}{dV}(T)|_{V=V_b}$. It is then normalized against $V_b = -50$ mV, namely $g_n(V_b, T) \equiv g(V_b, T)/g(-50\text{ mV}, T)$. Figure 4 displays $g_n(V_b, T)$ for two characteristic voltages: -21 and $+4$ mV. For $V_b = -21$ mV, they commonly exhibit a turning point around 60–70 K, indicative of the opening of a HG, in accordance with Figs. 2(a)–2(c). However, clear differences appear at low temperature: A rapid increase followed by plateauing below ~4 K for the FG versus gradual changes for FZs. For $V_b = +4$ mV, in contrast to the FZs, the FG conductance decreases monotonically down to 15–20 K, below which it turns up. This temperature corresponds to the resistive hump (Fig. 1) and hence its detailed analysis may help uncover the origin of the two activation gaps. If SmB_6 were a topologically trivial KI, the conductance within the HG would rapidly decrease to zero with decreasing temperature. Therefore, the low-temperature upturn must signify the emergence of the TSSs. Upon further lowering temperature, $g_n(+4\text{mV}, T)$ shows distinct changes among the three crystals, similarly to $g_n(-21\text{mV}, T)$. Again, these results show that the spectroscopic properties of the TSSs are quite different among the crystals despite the similarity in the bulk gap, as detailed below.

III. DISCUSSION

Our tunneling data reveal strong evidence for the interaction of the TSSs in SmB_6 with the SEs [28]. Then, the intriguing temperature dependence of both $g_n(+4\text{ mV}, T)$ and $R_n(T)$ might be caused by that of the SEs. The impact would be drastic at low temperature if, being a bosonic excitation, they undergo a Bose-Einstein condensation. Within this scenario, the rapid increase in $g_n(+4\text{ mV}, T)$ followed by plateauing might indicate that the TSSs in the FG become coherent as the SEs freeze out or condense. This is also suggested by the Pb coherence peaks becoming symmetric below ~4 K [Figs. 3(b) and 3(f)]. This is because, as the SEs condense, the aforementioned inelastic tunneling channel involving the absorption of SEs must be suppressed. In strong contrast to the FG, the TSSs in FZs do not exhibit such a distinct change in $g_n(+4\,\text{mV}, T)$ because the SEs remain uncondensed. Namely, the TSSs continue to interact with them and thus stay incoherent down to the lowest measurement temperature. These observations provide an answer to our earlier question: The low-temperature resistive slowdown behavior in FZs (Fig. 1) is still due to the TSSs rather than the in-gap states; however, $R_n(T)$ does not exhibit a clear plateau because the TSSs remain incoherent due to their continued interaction with the SEs. The condensation of SEs invoked here has also been reported in a muon spin rotation study on flux-grown SmB_6 crystals [43]. In addition, according to Valentine *et al.*'s report from Raman scattering spectroscopy on three SmB_6 crystals grown in similar batches to ours [44], the SE peak is sharp in the stoichiometric FG but becomes broader or even missing in Sm-deficient FZs despite the similar HG size as observed in our tunneling data. Thus, while the HG itself is not sensitive to low-level Sm deficiency, the properties of the SEs change drastically. Consequently, crystals with the Sm deficiency differing by as small an amount as 1% exhibit quite different behaviors in surface transport properties, in strong contrast to their weakly correlated counterparts [45]. Considering the growing interest in exciton physics on various condensed-matter platforms, including graphene [46,47] and transition-metal dichalcogenides [48], it is of great interest to further investigate the condensation of SEs in SmB_6. For instance, the measurement of d^2I/dV^2 may give the SE spectrum, analogously to the pairing-involved phonon spectrum in Pb [42]. The temperature dependence of such a spectrum may reveal the details underlying the exciton condensation process.

The sensitiveness of the topological nature to the Sm deficiency must affect many other properties in SmB_6. In particular, to resolve the enduring controversy over the origin of quantum oscillations in SmB_6 [9–12], more systematic studies

should be carried out with this aspect considered carefully. For instance, it is worthwhile to see how the signal indicative of the surface states [9] would change with the Sm deficiency. For a more microscopic understanding of our results, further theoretical investigation is necessary to study how the surface spectral density is modified due to the interaction with the SEs [34] in the presence of disorder, in particular the Sm deficiency [49,50]. The persistence of the HG up to 1% of Sm deficiency indicates that the translational invariance in the Kondo lattice, essential to the formation of coherent (hybridized) bands, may not yet be broken globally, still allowing the TSSs to emerge, albeit with quite different properties.

IV. CONCLUSION

In conclusion, our comparative tunneling studies on SmB_6 crystals show that the TSSs still exist for up to 1% of Sm deficiency, in line with the persistent bulk HG. However, their temperature evolution is distinctively different depending on the deficiency level as their interaction with the SEs varies drastically. In a stoichiometric crystal, the TSSs become coherent as the SEs condense, causing the resistance to exhibit a clear plateau at low temperature. In sharp contrast, the TSSs remain incoherent in Sm-deficient crystals due to their continued interaction with the SEs, thus showing a nonsaturating resistive behavior. This disorder sensitiveness of the topological nature in SmB_6, very likely TKIs in general, should be carefully considered when addressing the questions that remain open after a decade of intensive research. Theoretically, it will be important for future work to investigate how the influence of the SEs on the surface spectral density is modified by the Sm deficiency.

ACKNOWLEDGMENTS

The work at FSU and NHMFL was supported under Award No. NSF/DMR-1704712, and in part under Award No. NSF/DMR-1644779 and the State of Florida. The work at JHU was supported under Award No. DOE/BES EFRC DE-SC0019331. T.M.M. acknowledges JHU Catalyst Fund.

[1] X. L. Qi and S. C. Zhang, Rev. Mod. Phys. **83**, 1057 (2011).
[2] M. Z. Hasan and J. E. Moore, Annu. Rev. Condens. Matter Phys. **2**, 55 (2011).
[3] L. Fu, C. L. Kane, and E. J. Mele, Phys. Rev. Lett. **98**, 106803 (2007).
[4] P. S. Riseborough, Adv. Phys. **49**, 257 (2000).
[5] P. Coleman, *Handbook of Magnetism and Advanced Magnetic Materials* (Wiley, New York, 2007), pp. 95–148.
[6] M. Dzero, J. Xia, V. Galitski, and P. Coleman, Annu. Rev. Condens. Matter Phys. **7**, 249 (2016).
[7] M. Dzero, K. Sun, V. Galitski, and P. Coleman, Phys. Rev. Lett. **104**, 106408 (2010).
[8] J. W. Allen, Philos. Mag. **96**, 3227 (2016).
[9] G. Li, Z. Xiang, F. Yu, T. Asaba, B. Lawson, P. Cai, C. Tinsman, A. Berkley, S. Wolgast, Y. S. Eo, D. J. Kim, C. Kurdak, J. W. Allen, K. Sun, X. H. Chen, Y. Y. Wang, Z. Fisk, and L. Li, Science **346**, 1208 (2014).
[10] Z. Xiang, B. Lawson, T. Asaba, C. Tinsman, L. Chen, C. Shang, X. H. Chen, and L. Li, Phys. Rev. X **7**, 031054 (2017).
[11] B. S. Tan, Y. T. Hsu, B. Zeng, M. C. Hatnean, N. Harrison, Z. Zhu, M. Hartstein, M. Kiourlappou, A. Srivastava, M. D. Johannes, T. P. Murphy, J. H. Park, L. Balicas, G. G. Lonzarich, G. Balakrishnan, and S. E. Sebastian, Science **349**, 287 (2015).
[12] S. M. Thomas, X. X. Ding, F. Ronning, V. Zapf, J. D. Thompson, Z. Fisk, J. Xia, and P. F. S. Rosa, Phys. Rev. Lett. **122**, 166401 (2019).
[13] W. A. Phelan, S. M. Koohpayeh, P. Cottingham, J. A. Tutmaher, J. C. Leiner, M. D. Lumsden, C. M. Lavelle, X. P. Wang, C. Hoffmann, M. A. Siegler, N. Haldolaarachchige, D. P. Young, and T. M. McQueen, Sci. Rep. **6**, 20860 (2016).
[14] W. T. Fuhrman, J. R. Chamorro, P. A. Alekseev, J. M. Mignot, T. Keller, J. A. Rodriguez-Rivera, Y. Qiu, P. Nikolic, T. M. McQueen, and C. L. Broholm, Nat. Commun. **9**, 1539 (2018).
[15] M. M. Yee, Y. He, A. Soumyanarayanan, D.-J. Kim, Z. Fisk, and J. E. Hoffman, arXiv:1308.1085.
[16] Z. H. Zhu, A. Nicolaou, G. Levy, N. P. Butch, P. Syers, X. F. Wang, J. Paglione, G. A. Sawatzky, I. S. Elfimov, and A. Damascelli, Phys. Rev. Lett. **111**, 216402 (2013).
[17] J. Denlinger, J. W. Allen, J.-S. Kang, K. Sun, J.-W. Kim, J. H. Shim, B. I. Min, D.-J. Kim, and Z. Fisk, arXiv:1312.6637.
[18] E. Frantzeskakis, N. de Jong, B. Zwartsenberg, Y. K. Huang, Y. Pan, X. Zhang, J. X. Zhang, F. X. Zhang, L. H. Bao, O. Tegus, A. Varykhalov, A. de Visser, and M. S. Golden, Phys. Rev. X **3**, 041024 (2013).
[19] J. Jiang, S. Li, T. Zhang, Z. Sun, F. Chen, Z. R. Ye, M. Xu, Q. Q. Ge, S. Y. Tan, X. H. Niu, M. Xia, B. P. Xie, Y. F. Li, X. H. Chen, H. H. Wen, and D. L. Feng, Nat. Commun. **4**, 3010 (2013).
[20] C. H. Min, P. Lutz, S. Fiedler, B. Y. Kang, B. K. Cho, H. D. Kim, H. Bentmann, and F. Reinert, Phys. Rev. Lett. **112**, 226402 (2014).
[21] H. Miyazaki, T. Hajiri, T. Ito, S. Kunii, and S. I. Kimura, Phys. Rev. B **86**, 075105 (2012).
[22] M. Neupane, N. Alidoust, S. Y. Xu, T. Kondo, Y. Ishida, D. J. Kim, C. Liu, I. Belopolski, Y. J. Jo, T. R. Chang, H. T. Jeng, T. Durakiewicz, L. Balicas, H. Lin, A. Bansil, S. Shin, Z. Fisk, and M. Z. Hasan, Nat. Commun. **4**, 2991 (2013).
[23] N. Xu, P. K. Biswas, J. H. Dil, R. S. Dhaka, G. Landolt, S. Muff, C. E. Matt, X. Shi, N. C. Plumb, M. Radovic, E. Pomjakushina, K. Conder, A. Amato, S. V. Borisenko, R. Yu, H. M. Weng, Z. Fang, X. Dai, J. Mesot, H. Ding, and M. Shi, Nat. Commun. **5**, 4566 (2014).
[24] S. Rössler, T. H. Jang, D. J. Kim, L. H. Tjeng, Z. Fisk, F. Steglich, and S. Wirth, Proc. Natl. Acad. Sci. (USA) **111**, 4798 (2014).
[25] W. Ruan, C. Ye, M. H. Guo, F. Chen, X. H. Chen, G. M. Zhang, and Y. Y. Wang, Phys. Rev. Lett. **112**, 136401 (2014).
[26] X. H. Zhang, N. P. Butch, P. Syers, S. Ziemak, R. L. Greene, and J. Paglione, Phys. Rev. X **3**, 011011 (2013).
[27] See Supplemental Material at http://link.aps.org/supplemental/10.1103/PhysRevB.103.155125 for the discussion of materials

and methods (Sec. 1); characterization of the tunnel barrier (Sec. 2); comparison with photoemission results (Sec. 3); comparison with scanning tunneling and point-contact spectroscopies (Sec. 4); and independence of inelastic tunneling features on the counter-electrode (Sec. 5).

[28] W. K. Park, L. Sun, A. Noddings, D.-J. Kim, Z. Fisk, and L. H. Greene, Proc. Natl. Acad. Sci. (USA) **113**, 6599 (2016).

[29] F. Lu, J. Z. Zhao, H. M. Weng, Z. Fang, and X. Dai, Phys. Rev. Lett. **110**, 096401 (2013).

[30] V. Alexandrov, M. Dzero, and P. Coleman, Phys. Rev. Lett. **111**, 226403 (2013).

[31] J. Kim, K. Kim, C. J. Kang, S. Kim, H. C. Choi, J. S. Kang, J. D. Denlinger, and B. I. Min, Phys. Rev. B **90**, 075131 (2014).

[32] T. Takimoto, J. Phys. Soc. Jpn. **80**, 123710 (2011).

[33] W. T. Fuhrman, J. Leiner, P. Nikolic, G. E. Granroth, M. B. Stone, M. D. Lumsden, L. DeBeer-Schmitt, P. A. Alekseev, J. M. Mignot, S. M. Koohpayeh, P. Cottingham, W. A. Phelan, L. Schoop, T. M. McQueen, and C. Broholm, Phys. Rev. Lett. **114**, 036401 (2015).

[34] G. A. Kapilevich, P. S. Riseborough, A. X. Gray, M. Gulacsi, T. Durakiewicz, and J. L. Smith, Phys. Rev. B **92**, 085133 (2015).

[35] A. Arab, A. X. Gray, S. Nemsak, D. V. Evtushinsky, C. M. Schneider, D. J. Kim, Z. Fisk, P. F. S. Rosa, T. Durakiewicz, and P. S. Riseborough, Phys. Rev. B **94**, 235125 (2016).

[36] B. Gorshunov, N. Sluchanko, A. Volkov, M. Dressel, G. Knebel, A. Loidl, and S. Kunii, Phys. Rev. B **59**, 1808 (1999).

[37] P. Schlottmann, Phys. Rev. B **46**, 998 (1992).

[38] L. Sun, D. J. Kim, Z. Fisk, and W. K. Park, Phys. Rev. B **95**, 195129 (2017).

[39] D. J. Kim, J. Xia, and Z. Fisk, Nat. Mater. **13**, 466 (2014).

[40] P. Cheng, C. L. Song, T. Zhang, Y. Y. Zhang, Y. L. Wang, J. F. Jia, J. Wang, Y. Y. Wang, B. F. Zhu, X. Chen, X. C. Ma, K. He, L. L. Wang, X. Dai, Z. Fang, X. C. Xie, X. L. Qi, C. X. Liu, S. C. Zhang, and Q. K. Xue, Phys. Rev. Lett. **105**, 076801 (2010).

[41] T. Hanaguri, K. Igarashi, M. Kawamura, H. Takagi, and T. Sasagawa, Phys. Rev. B **82**, 081305(R) (2010).

[42] W. L. McMillan and J. M. Rowell, Phys. Rev. Lett. **14**, 108 (1965).

[43] K. Akintola, A. Pal, S. R. Dunsiger, A. C. Y. Fang, M. Potma, S. R. Saha, X. F. Wang, J. Paglione, and J. E. Sonier, npj Quantum Mater. **3**, 36 (2018).

[44] M. E. Valentine, S. Koohpayeh, W. A. Phelan, T. M. McQueen, P. F. S. Rosa, Z. Fisk, and N. Drichko, Physica B **536**, 60 (2018).

[45] J. G. Checkelsky, Y. S. Hor, M. H. Liu, D. X. Qu, R. J. Cava, and N. P. Ong, Phys. Rev. Lett. **103**, 246601 (2009).

[46] J. I. A. Li, T. Taniguchi, K. Watanabe, J. Hone, and C. R. Dean, Nat. Phys. **13**, 751 (2017).

[47] X. M. Liu, K. Watanabe, T. Taniguchi, B. I. Halperin, and P. Kim, Nat. Phys. **13**, 746 (2017).

[48] Z. F. Wang, D. A. Rhodes, K. Watanabe, T. Taniguchi, J. C. Hone, J. Shan, and K. F. Mak, Nature (London) **574**, 76 (2019).

[49] P. S. Riseborough, Phys. Rev. B **68**, 235213 (2003).

[50] M. Abele, X. Yuan, and P. S. Riseborough, Phys. Rev. B **101**, 094101 (2020).